Proceedings of the IASS 2024 Symposium
Redefining the Art of Structural Design
August 26-30, 2024, Zurich Switzerland
Philippe Block, Giulia Boller, Catherine DeWolf,
Jacqueline Pauli, Walter Kaufmann (eds.)

Enhancing Non-Linear Force Density Method through Combinatorial Equilibrium Modelling

Feifan HE*, Yinan XIAO[a], Yuchi SHEN[b], Hastia ASADI[c], Roland WÜCHNER[d], Pierluigi D'ACUNTO[c,e]

* Technical University of Munich, TUM School of Engineering and Design, Department of Architecture, Professorship of Structural Design
Arcisstraße 21, 80333 Munich, Germany
feifan.he@tum.de

[a] Technische Universität Braunschweig, Institute of Structural Design, Braunschweig
[b] Southeast University, School of Architecture, Nanjing
[c] Technical University of Munich, TUM School of Engineering and Design, Department of Architecture, Professorship of Structural Design, Germany
[d] Technische Universität Braunschweig, Institute of Statics and Dynamics, Braunschweig
[e] Technical University of Munich, TUM Institute for Advanced Study, Germany

Abstract

The Force Density Method (FDM) is an effective form-finding approach for exploring structural forms in equilibrium based on a given topology and under specified boundary conditions and external forces. Its nonlinear extension, the Non-Linear Force Density Method (NLFDM), was developed to enable structures to satisfy user-defined constraints. However, controlling the NLFDM is often challenging due to the difficulty in defining a suitable initial force density set that does not lead to degenerate results. In contrast, the Combinatorial Equilibrium Modelling (CEM) method enables an interactive and intuitive form-finding process for discrete networks, which offers a relatively high level of stability for designing mixed tension-compression structures. This paper reviews NLFDM and CEM and introduces an adaptive form-finding workflow for constrained discrete networks in static equilibrium that combines the two methods. CEM is employed to generate the initial structure and the force density set to be used as an input for NLFDM, thereby enhancing the controllability of the overall form-finding process; NLFDM ensures the speed and accuracy of the constraint-based optimization process. A case study is used to illustrate the proposed form-finding workflow.

Keywords: Form-finding, Non-Linear Force Density Method, Combinatorial Equilibrium Modelling, force density set, constraint-based structural optimization

1. Introduction

Form-finding allows the generation of new structural forms using either physical or digital models (Boller and D'Acunto [1]). This process entails determining the equilibrium shape of a structure for a given input topology and specified boundary conditions and applied loads. Different ways to solve the equilibrium problem for discrete networks lead to different form-finding methods within the realm of digital form-finding. Representative methods include the Force Density Method (Schek [2]), the Dynamic Relaxation Method (Barnes et al. [3]), the Updated Reference Strategy (Bletzinger et al. [4]), the Thrust Network Analysis (Block and John [5]), the Combinatorial Equilibrium Modelling (Ohlbrock and D'Acunto [6]) and Vector-based Graphic Statics (D'Acunto et al. [7]). To satisfy user-defined constraints, these methods are extended by integrating optimization processes. This paper focuses on

two geometric stiffness methods, namely the Force Density Method (FDM) with its extension, the Non-Linear Force Density Method (NLFDM) (Schek [2], Malerba et al. [8], Aboul-Nasr and Mourad [9]), and the Combinatorial Equilibrium Modelling (CEM), aiming to develop an adaptive form-finding workflow for constrained discrete networks.

By introducing the notion of force density, representing the force-to-length ratio, FDM addresses the form-finding of discrete networks by solving a set of linear equations. For a given topological diagram $\mathbf{T_F}$ (Figure 1 left), which provides the connectivity of different members, nodes are categorized into two groups: fixed nodes $\mathbf{V_f}$ and free nodes $\mathbf{V_v}$. Connections between nodes are represented as edges. Based on $\mathbf{T_F}$, given the coordinates $\boldsymbol{C_f}$ of the fixed nodes $\mathbf{V_f}$ and the external forces $\boldsymbol{P_v}$ applied to the free nodes $\mathbf{V_v}$, FDM generates the structural form $\mathbf{F_F}$ (Figure 1 right) after assigning an initial force density set $\boldsymbol{q}$ to all edges. NLFDM is used when user-defined constraints, like lengths and force magnitudes of the edges, are considered. NLFDM deals with multi-constraints form-finding problems with the help of a gradient-based optimization algorithm. The speed and accuracy of this method are guaranteed by directly employing the exact mathematical expression for gradient-based optimization calculations.

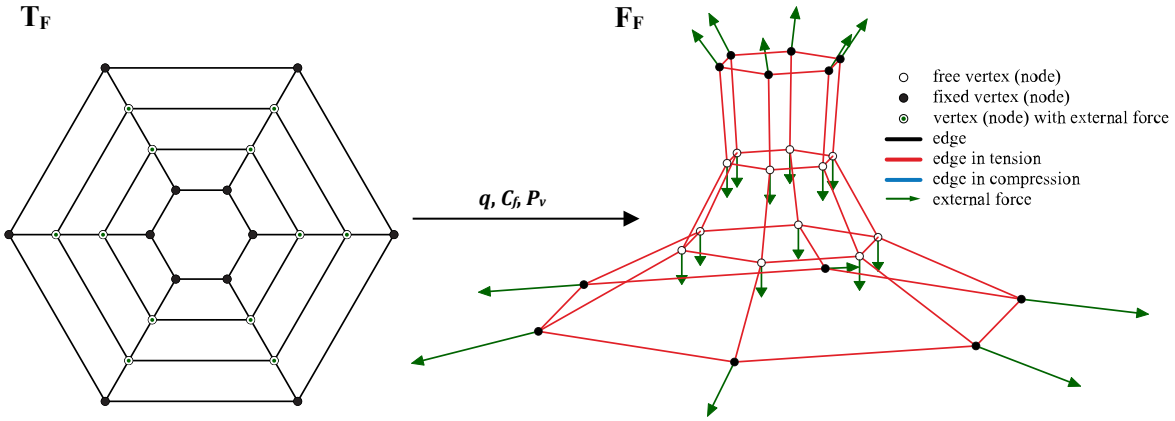

Figure 1: FDM topological diagram of a truncated pyramid-like structure (left); result of the form-finding process based on the FDM (right)

In contrast, CEM (Ohlbrock and D'Acunto [6]) introduces additional information on the topological diagram $\mathbf{T_C}$ (Figure 2 left) to guide the form-finding process for discrete networks. In $\mathbf{T_C}$, nodes are categorized into three types: origin nodes $\mathbf{V_o}$, normal nodes $\mathbf{V_n}$, and support nodes $\mathbf{V_s}$. Edges are categorized into trail edges $\mathbf{E_t}$ and deviation edges $\mathbf{E_d}$, and the user can freely assign the combinatorial state (tension or compression) of their internal forces. The polylines that originate from an origin vertex and terminate at a support vertex are called trails, and the segments that form them are the trail edges $\mathbf{E_t}$. Deviation edges $\mathbf{E_d}$ link nodes on different trails. Based on $\mathbf{T_C}$, under the external forces $\boldsymbol{P}$ on the nodes, the structural form $\mathbf{F_C}$ (Figure 2 right) is constructed sequentially from the position $\boldsymbol{C_o}$ of the origin nodes $\mathbf{V_o}$ by assigning the trail lengths $\boldsymbol{\lambda}$, and deviation force magnitudes $\boldsymbol{\mu}$ to the $\mathbf{E_t}$ and $\mathbf{E_d}$, respectively. It is worth mentioning that a constraint plane ($\boldsymbol{CPL}$) for every node can replace the trail lengths $\boldsymbol{\lambda}$ as part of the input parameters in CEM. As the form-finding process of CEM follows a linear sequence from the $\mathbf{V_o}$ to the $\mathbf{V_s}$, the form-finding process presents a high level of stability, especially for a complex combination of tension-compression internal forces (Ohlbrock et al. [10]). Two extensions of the CEM have been developed to solve structures with user-defined constraints. One extension uses the finite difference approximation method to calculate the gradient and then employs a gradient-based local optimization algorithm for optimization (Ohlbrock et al. [11]). While this method is straightforward to implement, it can suffer from numerical instability because the choice of step size in the finite difference approximation can significantly influence the accuracy of gradients. To address this problem, the second extension (Pastrana et al. [12]) utilizes the Automatic Differentiation (AD) method for gradient calculations, resulting in a quicker and more precise optimization process.

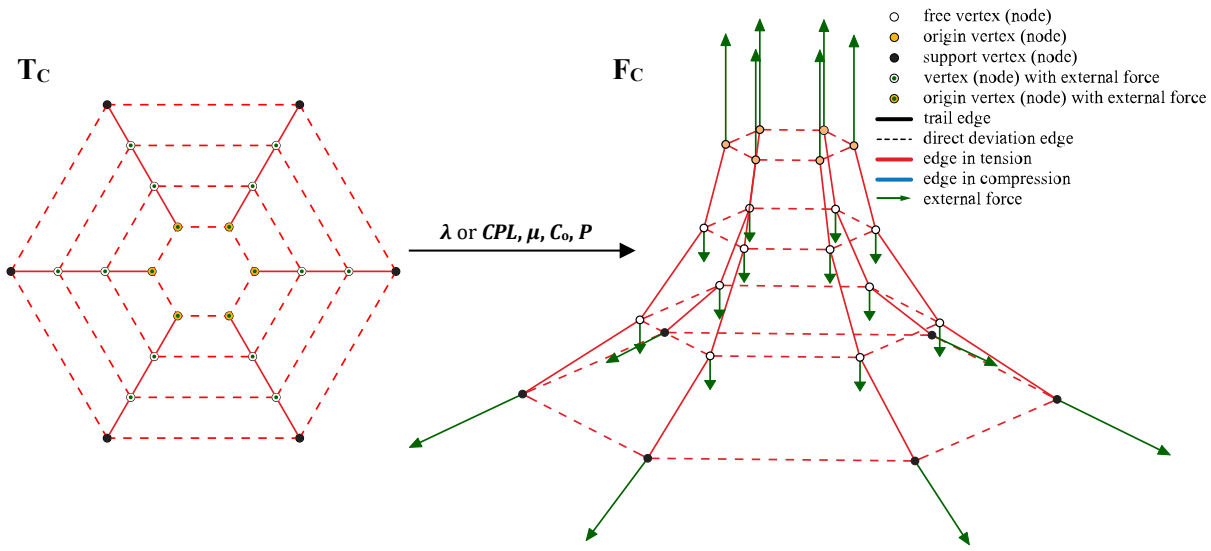

Figure 2: CEM topological diagram of a truncated pyramid-like structure (left); result of the form-finding process based on the CEM (right)

NLFDM and the extended CEM (Pastrana et al. [12]) are effective form-finding methods for constrained discrete networks. However, utilizing NLFDM or the extended CEM to achieve a fast, accurate, and user-controllable optimization process could be challenging. Although the use of symbolic differentiation (SD) has enhanced the speed and accuracy of NLFDM, designers might face challenges in defining an initial set of force densities that meets user expectations for subsequent NLFDM control (Malerba et al. [8]). This difficulty arises from the abstract concept of force density and the highly non-linear correlation between the generated structural forms and the initial force density set (Ohlbrock and D'Acunto [6], Veenendaal and Block [13]). In the extended CEM, while CEM provides an intuitive and interactive form-finding process for defining the initial structure, its sequential and iterative nature fails to make the constrained form-finding process particularly computationally efficient, especially compared to NLFDM (Pastrana et al. [12]). Given the complementary characteristics of NLFDM and CEM, this research combines these two methods to develop a controllable, fast, and accurate form-finding workflow (CEM+NLFDM) for constrained discrete networks.

2. Method

2.1. Workflow

The proposed CEM+NLFDM form-finding workflow is illustrated in Figure 3. The design requirements consist of two categories: 1. constraints (e.g., the length of the member, the force of the member, and the reaction force acting on the fixed nodes), which can be satisfied exactly, and 2. desired objectives (**DO**) (e.g., a target shape) which depend on the designer's needs. Based on the design structural topology (**T**), desired objectives (**DO**), and the prescribed values $\boldsymbol{R_p}$ for constraint parameters, the form-finding process is as follows: in the first step, the CEM structural topological diagram ($\mathbf{T_C}$) is determined based on **T**. The designer manually adjusts the input parameters in CEM to generate an initial structure that aligns with **DO**. Moreover, the squared norm of the weighted difference L between the actual constraint parameters value $\boldsymbol{R}$ and the prescribed values $\boldsymbol{R_p}$ (determined by Equation 1 with weighting factors $\boldsymbol{\omega}$) is ensured to remain below a user-defined finite threshold ε_0. Then, the force density set $\boldsymbol{q_0}$ computed from this initial structure serves as the input force density set for NLFDM. In the second step, based on the structural topological diagram ($\mathbf{T_F}$) determined from **T**, NLFDM is applied to guarantee the structure satisfies the constraints precisely. If the final structure fails to fulfill the **DO** (such as substantial changes in overall form after optimization) or if L is greater than the threshold $\varepsilon_1 \ll \varepsilon_0$, the designer needs to redefine a smaller ε_0 to bring the initial structure closer to the fulfillment of the constraints. Following this adjustment, the above steps are repeated iteratively until a solution is found.

$$L = \left\| \boldsymbol{\omega}\left(\boldsymbol{R} - \boldsymbol{R_p}\right) \right\|^2 \tag{1}$$

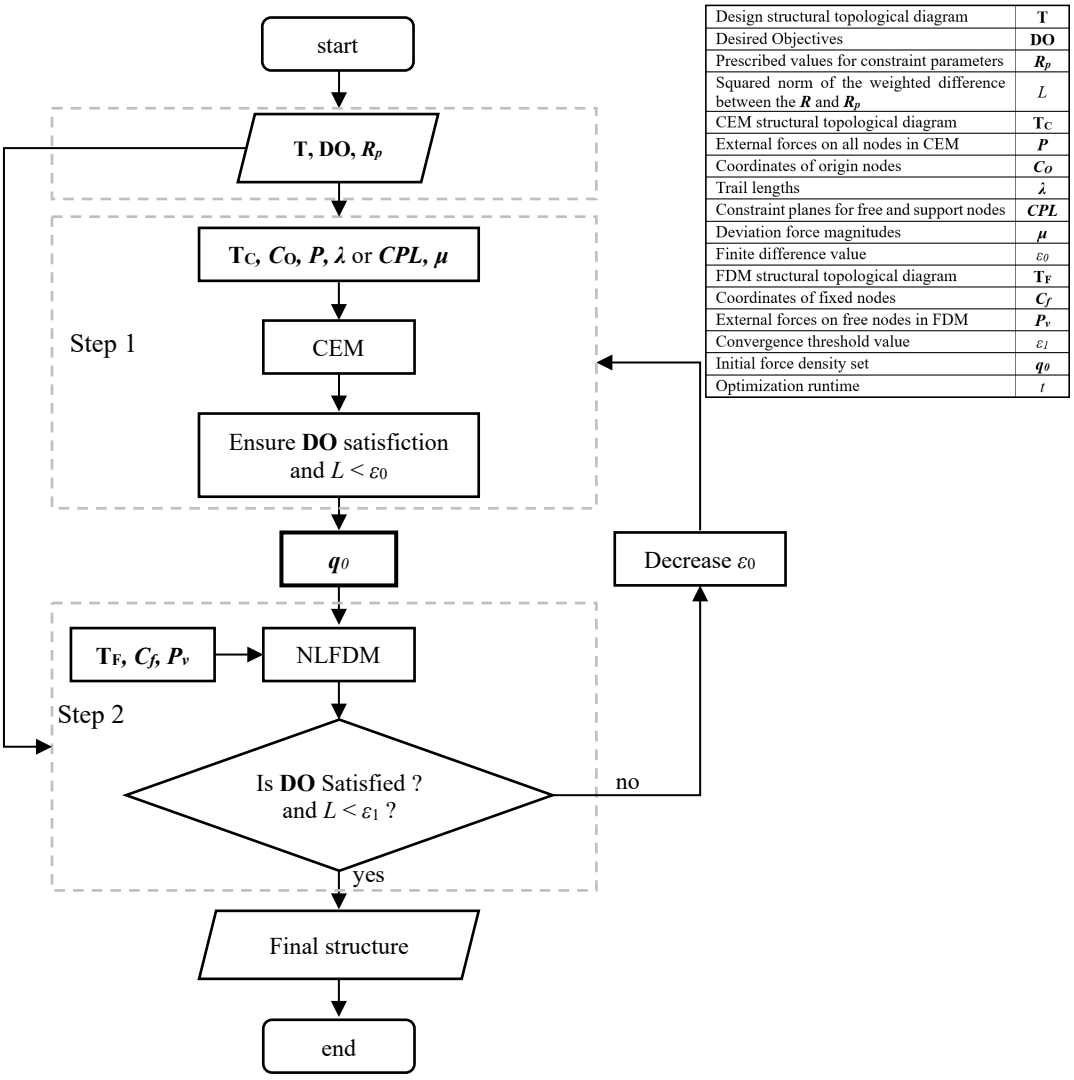

Design structural topological diagram	**T**
Desired Objectives	**DO**
Prescribed values for constraint parameters	R_p
Squared norm of the weighted difference between the R and R_p	L
CEM structural topological diagram	T_C
External forces on all nodes in CEM	P
Coordinates of origin nodes	C_O
Trail lengths	λ
Constraint planes for free and support nodes	CPL
Deviation force magnitudes	μ
Finite difference value	ε_0
FDM structural topological diagram	T_F
Coordinates of fixed nodes	C_f
External forces on free nodes in FDM	P_v
Convergence threshold value	ε_1
Initial force density set	q_0
Optimization runtime	t

Figure 3: CEM+NLFDM form-finding workflow

2.2. Optimization method and constraints

In optimization problems, the choice of initial values and the method for gradient calculations are crucial factors that significantly influence the process's controllability, speed, and accuracy. In the proposed workflow, CEM facilitates an interactive manual search for an appropriate initial force density set, aligning with the desired design objectives by directly adjusting its input parameters, thereby ensuring comprehensive control over the entire process. NLFDM enhances the speed and accuracy of the optimization process by utilizing exact mathematical expressions to compute gradients.

Plane constraints (***CPL***) are part of the input parameters of CEM form-finding process to anchor nodes onto designer-defined planes. To ensure these constraints are preserved in the final optimized result, ***CPL*** is introduced into NLFDM in compliance with Newton's method. As shown by Schek [2], the constrained problems are solved using Newton's method to find the roots of Equation 2. The plane constraint function is represented by Equation 3. The gradient of this function with respect to $\boldsymbol{q}$ is obtained using Equation 4 in which $\frac{\partial x_i}{\partial \boldsymbol{q}}$, $\frac{\partial y_i}{\partial \boldsymbol{q}}$, $\frac{\partial z_i}{\partial \boldsymbol{q}}$ are provided by Aboul-Nasr and Mourad [9].

$$\boldsymbol{g} = \boldsymbol{R} - \boldsymbol{R_p} = \boldsymbol{0} \tag{2}$$

$$g_i = A_i x_i + B_i y_i + C_i z_i + D_i = 0 \tag{3}$$

$$\frac{\partial g_i}{\partial \boldsymbol{q}} = A_i \frac{\partial x_i}{\partial \boldsymbol{q}} + B_i \frac{\partial y_i}{\partial \boldsymbol{q}} + C_i \frac{\partial z_i}{\partial \boldsymbol{q}} \tag{4}$$

where g_i, the i-th constraint equation in $\boldsymbol{g}$, denotes that the i-th target node whose coordinate is (x_i, y_i, z_i), lies in the i-th plane, characterized by plane coefficients A_i, B_i, C_i, and D_i.

3. Implementation: a spiral staircase

Figure 4 shows the configuration of a spiral staircase with 20 steps, taken here as a case study to illustrate the CEM+NLFDM form-finding workflow. The external force applied on each free node is 1kN. Three types of constraints are prescribed: each step edge is 1.0 meters wide; the height h_j of j-th point v_j is given by Equation 5 to ensure the step edges lie in horizontal planes (Φ_1, Φ_2, …, Φ_{19}) evenly distributed along the staircase's height; and nodes v_0, v_{20}, v_{21}, and v_{41} are fixed with coordinates specified in Table 1. These constraints are collected in $\boldsymbol{R_p}$. Besides, the footprint area of the staircase is limited to the surface Π (**DO**) (Figure 4b). To verify the effectiveness of CEM+NLFDM, we compared it with NLFDM alone and the extended CEM alone regarding the form-finding process's controllability and optimization runtime (t). All the weighting factors in $\boldsymbol{\omega}$ are set to 1. All codes were executed on an Intel i9-10900K CPU.

$$h_j = \begin{cases} -0.15j + 3 & j\epsilon\{1, 2, 3, \dots, 19\} \\ -0.15(j-21) + 3 & j\epsilon\{22, 23, 24, \dots, 40\} \end{cases} \tag{5}$$

3.1. Form-finding using CEM + NLFDM

Using CEM+NLFDM, the staircase form is obtained through the following steps: Initially, the CEM topological diagram $\mathbf{T_C}$ is determined, as shown in Figure 5a. ε_0 is set to 100. By adjusting the input parameters of the CEM layer by layer, the CEM sequentially builds the overall structure (Figure 5b) over surface Π, ensuring that the **DO** can be effectively achieved. The positions of fixed nodes v_0 and v_{21} are designated as origin nodes. Apart from the vertical force (1kN) on each free node, the external force $\boldsymbol{P_O}$ applied to the origin nodes is shown in Table 2. The deviation force magnitudes $\boldsymbol{\mu}$ is listed in Table 3. The height of the constraint horizontal plane (***CPL***) for each free node in CEM is determined by Equation 5. In the CEM result (Figure 5b), the L value is 98.27, which is smaller than ε_0. Subsequently, the FDM topological diagram $\mathbf{T_F}$ (Figure 4a), the derived force density set $\boldsymbol{q_0}$ (Figure 5c), the coordinates $\boldsymbol{C_f}$ of fixed nodes v_0, v_{20}, v_{21}, and v_{41}, and the external load $\boldsymbol{P_v}$ (each force is 1kN) serve as input parameters for NLFDM. Newton's method is the optimization algorithm with a convergence threshold ε_1 set at 1×10^{-6}. The plane constraint (Equations 3 and 4) and length constraint (Schek [2]) are introduced into NLFDM. The optimization process concludes in 0.029 seconds. The final result (Figure 5d) confirms compliance with constraints and **DO** and retains a form closely aligned with the initial structure.

3.2. Form-finding using NLFDM alone

A second experiment is conducted to compare CEM+NLFDM with NLFDM alone. Newton's method is used as the optimization algorithm, incorporating the plane constraint (Equations 3 and 4) and length constraint (Schek [2]). The optimization convergence threshold is set to 1×10^{-6}. Within the NLFDM form-finding process, adjusting the force density value in each edge individually to achieve the desired form poses a considerable challenge. Therefore, as shown in Figure 4a, all edges are categorized into three groups (Chord 1, Chord 2, Step) according to their respective static role in the staircase. The same force density value is uniformly applied to all edges in each group. Table 4 lists four initial force density sets for NLFDM related to four case studies. Together with $\boldsymbol{C_f}$ and $\boldsymbol{P_v}$, the corresponding initial and final structures are calculated (Figure 6).

As shown in Figure 6, increasing the force density in Chord 1 from 30 kN/m (Case 1) to 50 kN/m (Case 2) and then to 70 kN/m (Case 3) brings about substantial changes in the resulting form (Figure 6b, 6d and 6f). This demonstrates the significant non-linearity of the method. Additionally, although NLFDM can ensure all the constraints are satisfied, the projection geometries in all three cases exceed the design boundary Π, indicating the challenge of achieving **DO** by adjusting the initial force density set. Regarding the speed of the optimization process (Table 5), all four cases are slower compared to the CEM+NLFDM case. This is because the tentative choice of the initial force density set causes the NLFDM to easily converge to local optima, making NLFDM less computationally efficient than CEM+NLFDM. Therefore, identifying suitable initial force density values in NLFDM for the three

groups of edges to meet designers' requirements and achieve a fast form-finding process poses a challenge. At the same time, it is worth mentioning that Case 4, with an initial force density set closely matching the distribution in Figure 5c, produces the most reasonable final result that meets all the requirements and achieves the highest speed among the four NLFDM cases. In summary, utilizing CEM to search for the initial force density set is quick and efficient, unlike trial-and-error adjustments to different force density sets as in NLFDM alone. Furthermore, while grouping edges can greatly simplify searching for a reasonable form compared to individual adjustment of each edge's force density, designers might miss numerous opportunities to explore novel design solutions.

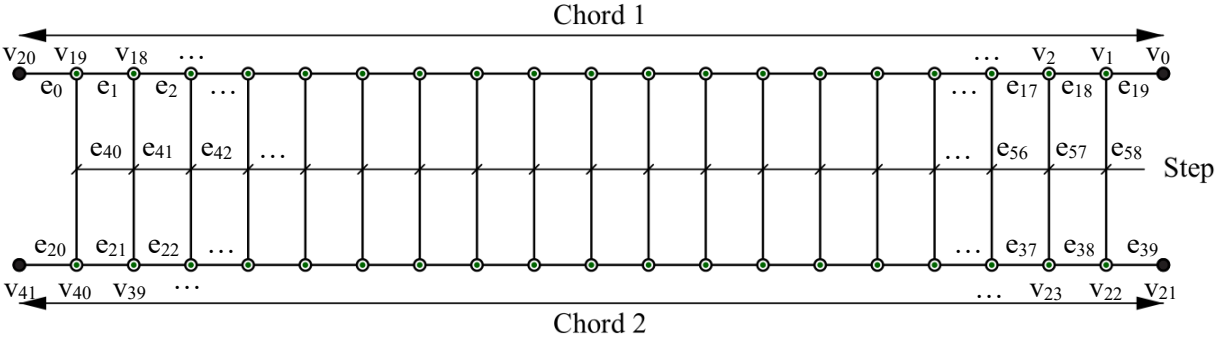

(a) Topology (**T**) of the staircase: edges are grouped into three categories: Chord 1, Chord 2, and Step

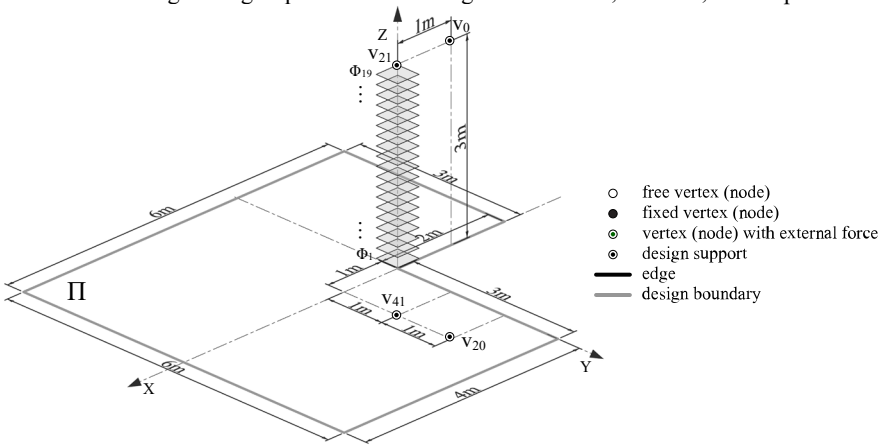

(b) Constraints and desired objectives (i.e., **DO**: limitation surface Π)

Figure 4: Configuration of the staircase

Table 1: Coordinates of the fixed nodes v_0, v_{20}, v_{21}, and v_{41} [m]

	C_x	C_y	C_z
v_0	-1.00	0.00	3.00
v_{20}	1.00	2.00	0.00
v_{21}	0.00	0.00	3.00
v_{41}	1.00	1.00	0.00

Table 2: External forces $\boldsymbol{P_O}$ applied to origin nodes [kN]

	P_x	P_y	P_z
v_0	142.4	63.6	65.1
v_{21}	-114.5	-67.4	-104.6

Table 3: Deviation force magnitudes $\boldsymbol{\mu}$ [-kN]

e_{58}	e_{57}	e_{56}	e_{55}	e_{54}	e_{53}	e_{52}	e_{51}	e_{50}	e_{49}	e_{48}	e_{47}	e_{46}	e_{45}	e_{44}	e_{43}	e_{42}	e_{41}	e_{40}
39.1	40.2	41.2	42.3	43.4	44.5	45.5	46.6	47.7	48.8	49.8	50.9	52.0	53.0	54.1	55.2	56.3	57.3	58.4

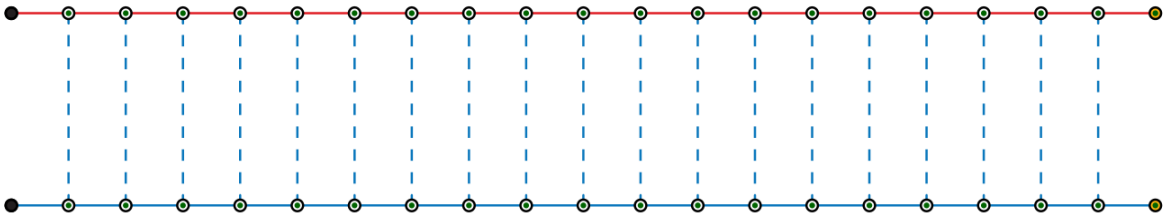

(a) CEM topology of the staircase

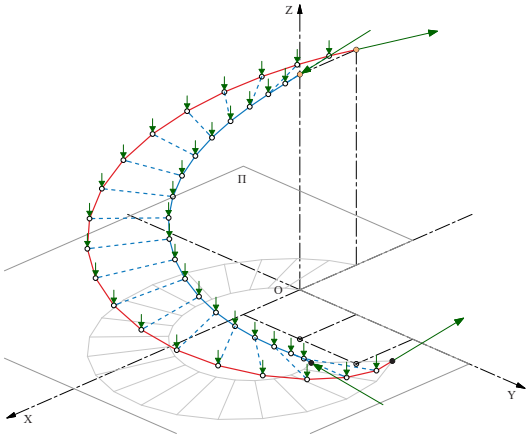

(b) Initial structural form generated by CEM

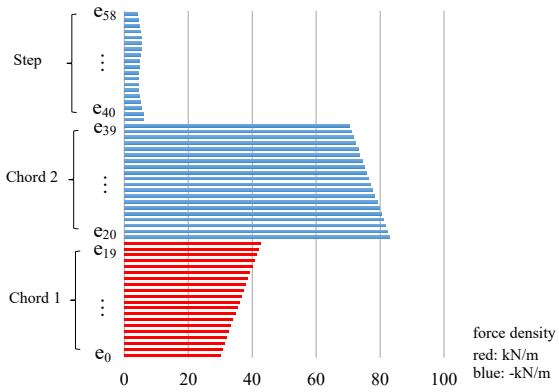

(c) Force density distribution in the initial structure

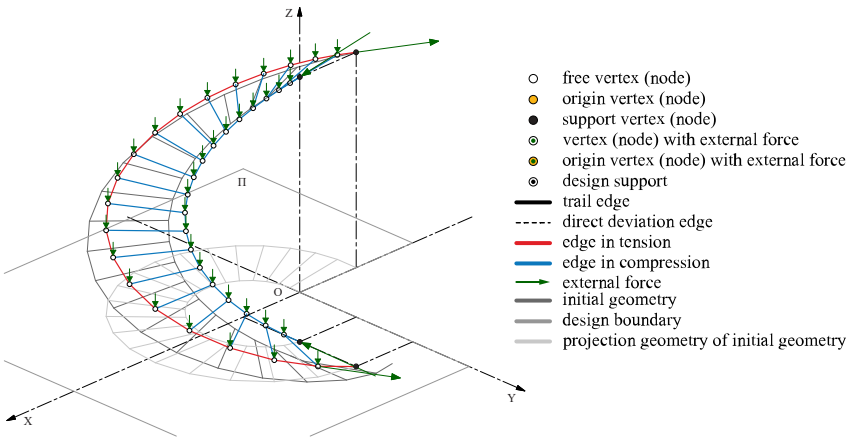

(d) Final structural form optimized by NLFDM (t = 0.029s)

Figure 5: Form-finding based on CEM+NLFDM workflow

Table 4: Four initial force density sets for NLFDM [kN/m]

	Chord 1	Chord 2	Step
Case 1	30	-70	-10
Case 2	50	-70	-10
Case 3	70	-70	-10
Case 4	40	-70	-5

3.3. Form-finding using CEM alone

For a comparative analysis between NLFDM and extended CEM in which AD is utilized for gradient calculations, the same initial structure (Figure 5b) is used as the starting point of the optimization process of extended CEM. The plane, length, and node position constraints (Pastrana et al. [11]) are added to the optimization process in the extended CEM. A convergence threshold of 1×10^{-6} is set, with SLSQP (Kraft [14]) serving as the optimization algorithm. The optimization result is shown in Figure 7. Constraints and **DO** are successfully satisfied. However, the optimization process takes 30.8 seconds to converge, which is significantly slower than CEM+NLFDM.

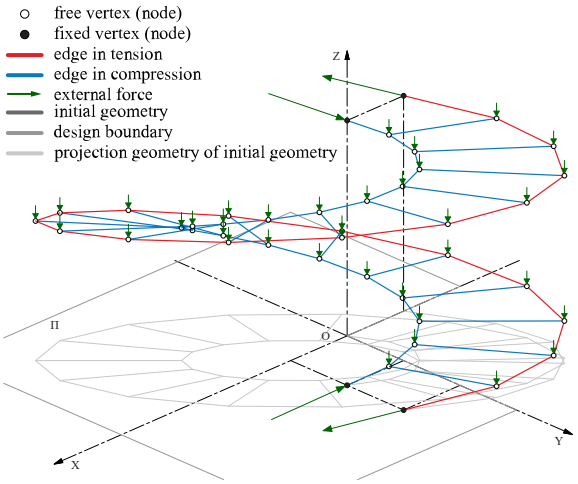

(a) Case 1: initial structural form

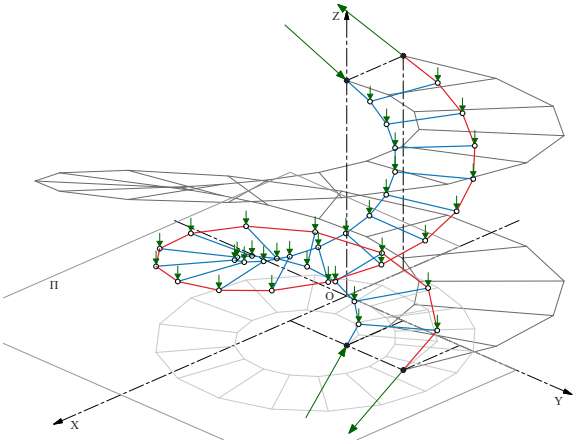

(b) Case 1: structural form after optimization (t = 0.043s)

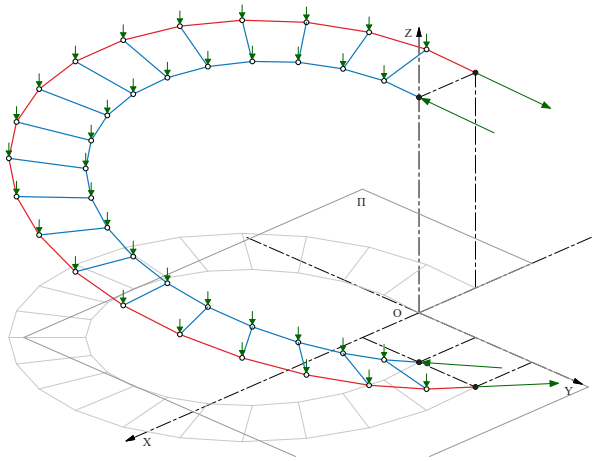

(c) Case 2: initial structural form of Case 2

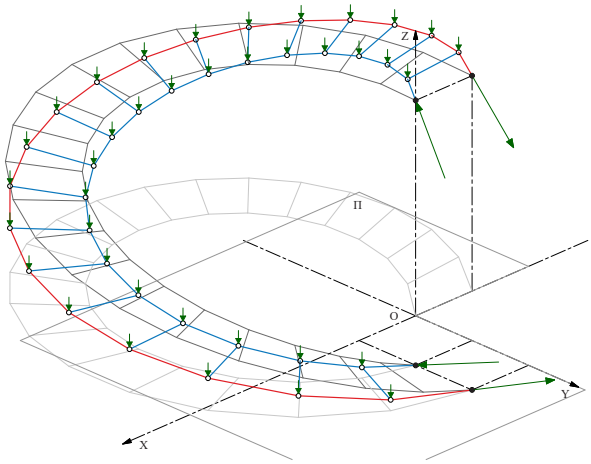

(d) Case 2: structural form after optimization (t = 0.232s)

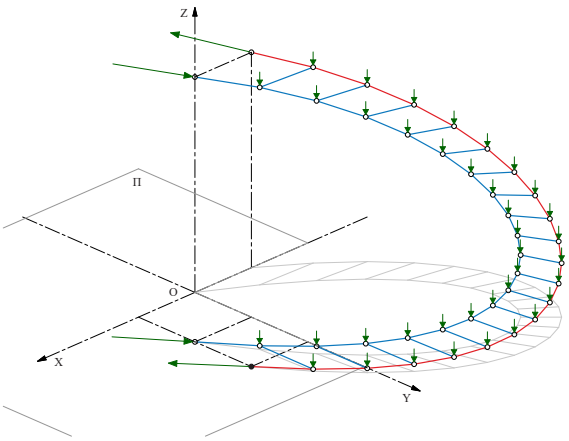

(e) Case 3: initial structural form

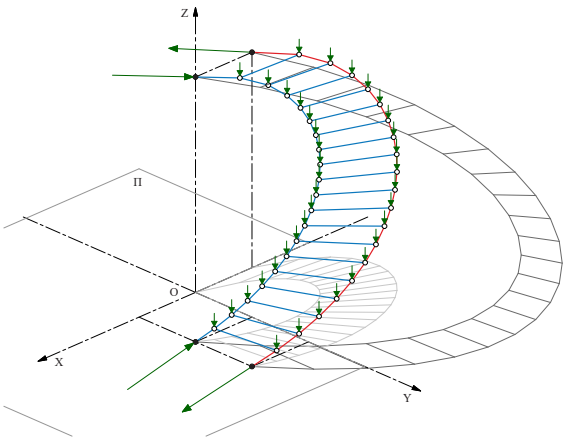

(f) Case 3: structural form after optimization (t = 3.4s)

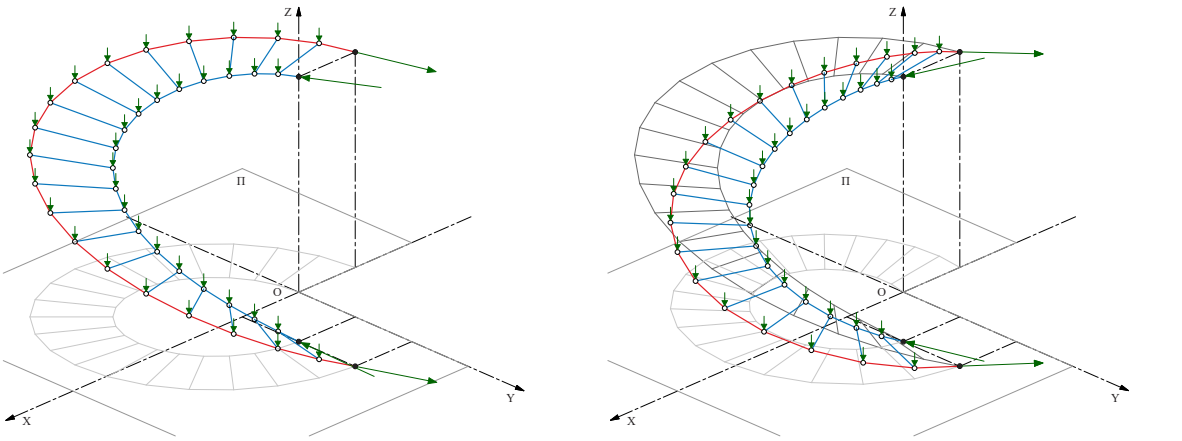

(g) Case 4: initial structural form (h) Case 4: structural form after optimization (t = 0.035s)

Figure 6: Four initial structural forms and corresponding NLFDM form-finding results

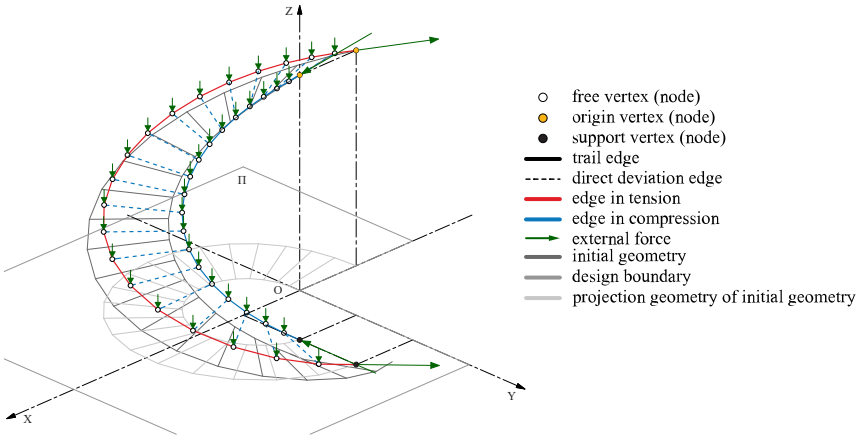

Figure 7: Result of the form-finding based on the extended CEM (t = 30.8s)

Table 5: Optimization runtime (t) of the CEM+NLFDM, NLFDM, and extended CEM upon convergence [s]

	CEM+NLFDM	NLFDM				extended CEM
		Case 1	Case 2	Case 3	Case 4	
t	0.029	0.043	0.232	3.4	0.035	30.8

4. Conclusion

This paper presented an adaptive form-finding workflow for constrained discrete networks in the conceptual design phase based on CEM and NLFDM. In this workflow, CEM is used to generate a user-expected initial structure. Then, NLFDM ensures precise satisfaction of the constraints by utilizing the force density set computed from this initial structure as the initial values of the NLFDM optimization process. Compared to the NLFDM alone, this workflow offers greater controllability as CEM serves as the initial structure generator to align with the design requirements. At the same time, NLFDM tends to be faster and more accurate than the extended CEM alone. As a result, this adaptive form-finding workflow facilitates a controllable, rapid, and accurate form-finding process for constrained discrete networks. Future research will be conducted on extending current work with the Finite Element Method (FEM) (Wan et al. [15], Brütting et al. [16]). Additionally, new optimization constraints, targets, and algorithms will be introduced to enhance this workflow's integrity, automation, and controllability.

Acknowledgments

Feifan He acknowledges the support of China Scholarship Council program (No.202206120041).

Yinan Xiao received support from Matthäi - Stiftung, Germany.

Yuchi Shen received support by the Natural Science Foundation of China (NSFC#52208010) and the China Postdoctoral Science Foundation (#2022M720716).

References

[1] G. Boller and P. D'Acunto. "Structural design via form finding: Comparing Frei Otto, Heinz Isler and Sergio Musmeci." *History of Construction Cultures*, vol. 2, pp. 431-438, 2021.

[2] H.-J. Schek, "The force density method for form finding and computation of general networks." *Computer Methods in Applied Mechanics and Engineering,* vol. 3, no. 1, pp. 115-134, 1974.

[3] M. Barnes, P. Dune, M. Haase, and J. Orkisz. "Form finding and analysis of tension structures by dynamic relaxation." *International Journal of Space Structure,* vol. 14, no. 2, pp. 89-104, 1999.

[4] K.-U. Bletzinger and E. Ramm, "A general finite element approach to the form finding of tensile structures by the updated reference strategy." *International Journal of Space Structure,* vol. 14, no. 2, pp. 131-145, 1999.

[5] P. Block, and O. John, "Thrust network analysis: a new methodology for three-dimensional equilibrium." *Journal of the International Association for Shell and Spatial Structures,* vol. 48, no. 3, pp. 167-173, 2007.

[6] P. O. Ohlbrock and P. D'Acunto, "A computer-aided approach to equilibrium design based on graphic statics and combinatorial variations." *Computer-Aided Design,* vol. 121, p. 102802, 2020.

[7] P. D'Acunto, J.-P. Jasienski, P.O. Ohlbrock, C. Fivet, J. Schwartz, and D. Zastavni, "Vector-based 3D graphic statics: A framework for the design of spatial structures based on the relation between form and forces." *International Journal of Solids and Structures*. vol. 167, pp. 58–70, 2019.

[8] P. G. Malerba, M. Patelli, and M. Quagliaroli, "An extended force density method for the form finding of cable systems with new forms." *Structural Engineering and Mechanics,* vol. 42, no. 2, pp. 191-210, 2012.

[9] G. Aboul-Nasr and S. A. Mourad, "An extended force density method for form finding of constrained cable nets." *Case Studies in Structural Engineering,* vol. 3, pp. 19-32, 2015.

[10] P. O. Ohlbrock, P. D'Acunto. J.-P. Jasienski, and C. Fivet, Vector-based 3D graphic statics (part III): designing with Combinatorial Equilibrium Modelling. *In: Proceedings of IASS annual symposia*, Tokoyo, Japan, 2016, pp.1-10.

[11] P. O. Ohlbrock, P. D'Acunto, J.-P. Jasienski, and C. Fivet, Constraint-Driven Design with Combinatorial Equilibrium Modelling. *In: Proceedings of IASS annual symposia*, Hamburg, Germany, 2017, pp.1-10.

[12] R. Pastrana, P. O. Ohlbrock, T. Oberbichler, P. D'Acunto, and S. Parascho, "Constrained form-finding of tension-compression structures using automatic differentiation." *Computer-Aided Design,* vol. 155, p. 103435, 2023.

[13] D. Veenendaal and P. Block, "An overview and comparison of structural form finding methods for general networks." *International Journal of Solids and Structures,* vol. 49, no. 26, pp. 3741-3753, 2012.

[14] D. Kraft, "A software package for sequential quadratic programming." *Tech. Rep. DFVLR-FB 88-28, DLR German Aerospace Center — Institute for Flight Mechanics,* 1988.

[15] Z. Wan, P. O. Ohlbrock, P. D'Acunto, Z. Cao, F. Fan, and J. Schwartz, "A form-finding approach for the conceptual design of air-supported structures using 3D graphic statics. " *Computers & Structures,* vol. 243, no. 106401, 2021.

[16] J. Brütting, P. O. Ohlbrock, J. Hofer, and P. D'Acunto, "Stock-constrained truss design exploration through combinatorial equilibrium modeling. " *International Journal of Space Structures*, vol. 36, no.4, pp. 253-269, 2021.